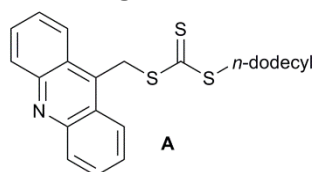


Electronic Supporting Information
for

Construction of DNA–polymer hybrids using intercalation interactions

Thomas R. Wilks, Anaïs Pitto-Barry, Nigel Kirby, Eugen Stulz and Rachel K. O'Reilly

Use of an alternative acridine-containing CTA

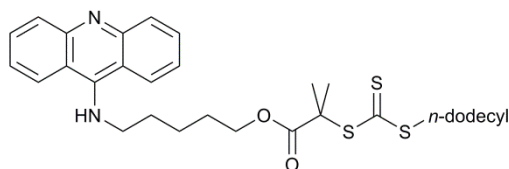


The reversible addition–fragmentation chain transfer (RAFT) polymerisation of several monomers (see Table S1) was attempted using the acridine-containing chain transfer agent (CTA) **A**. However, under no conditions was control achieved – this was hypothesised to be because the methyl acridine radical is too stable to undergo efficient reinitiation (a key step of the RAFT process).

Table S1. Details of the polymerisations attempted with CTA **A**. NIPAM = N-isopropylacrylamide; MA = methyl acrylate.
*Determined by integration of the SCH₂ group to the OCH₃ group. †Determined by THF SEC using PMMA calibration standards; two peaks were observed, which were analysed separately. ‡Part of the distribution fell outside the calibration limits – these numbers are therefore likely to be inaccurate.

Monomer	Conversion after 24 h	M _n ^{NMR} / Da*	M _n ^{SEC} / Da [†]	Đ [‡]
Styrene	0 %	-	-	-
NIPAM	0 %	-	-	-
MA	13 %	2 700	3 500 163 000 [‡]	1.12 1.39 [‡]

RAFT polymerisation using CTA **1**



The controlled RAFT polymerisation of N-isopropylacrylamide (NIPAM), 4-acryloyl morpholine (4-AM), N,N-dimethylacrylamide (DMA) and tri(ethylene glycol) methyl ether acrylate (TEGA) was achieved using CTA **1** as described in the main paper (Scheme S1). Figure S1 shows a ¹H NMR spectrum of **P2**; the peaks due to the acridine end group, polymer backbone and trithiocarbonate group are all visible. The presence of the acridine group was also confirmed by size exclusion chromatography (SEC) using an inline UV-vis detector set to collect at 309 nm (characteristic of the

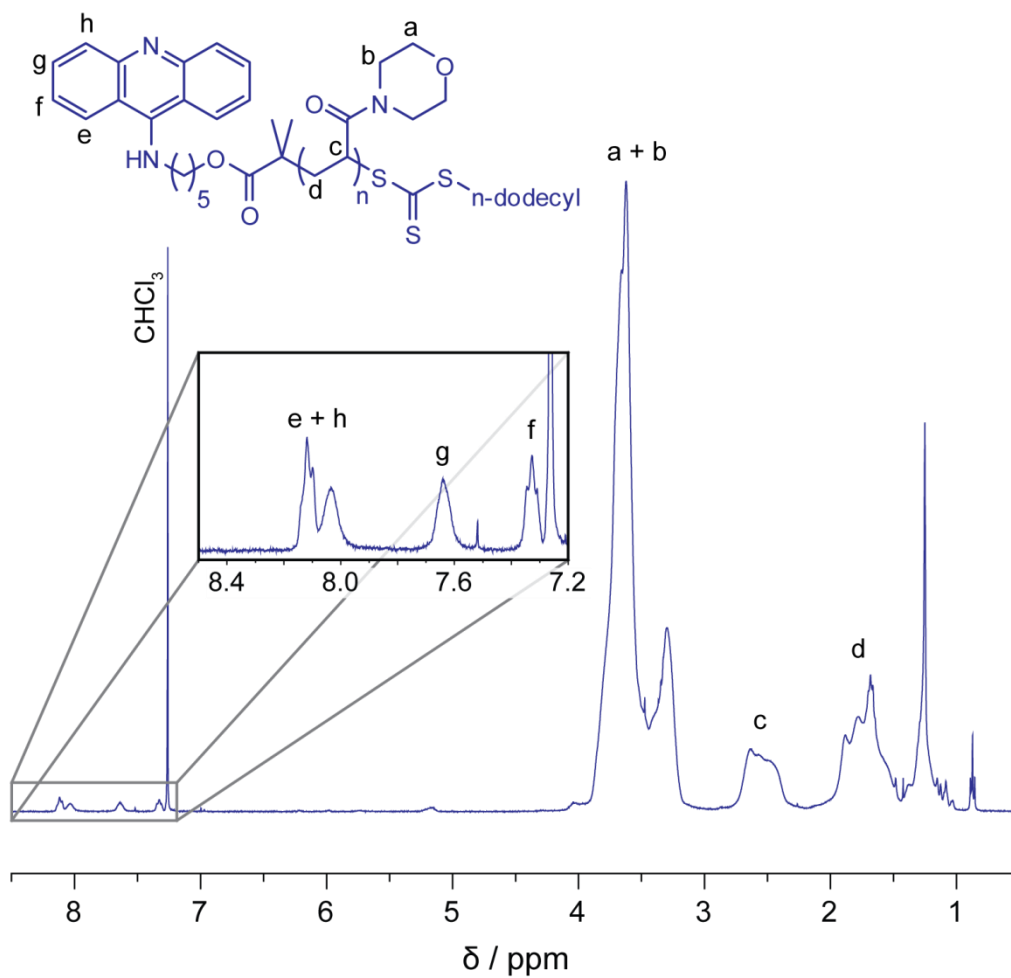


Figure S1. ^1H NMR spectrum of **P2** showing the peaks due to the acridine and trithiocarbonate end groups and the polymer backbone. Solvent: CDCl_3 .

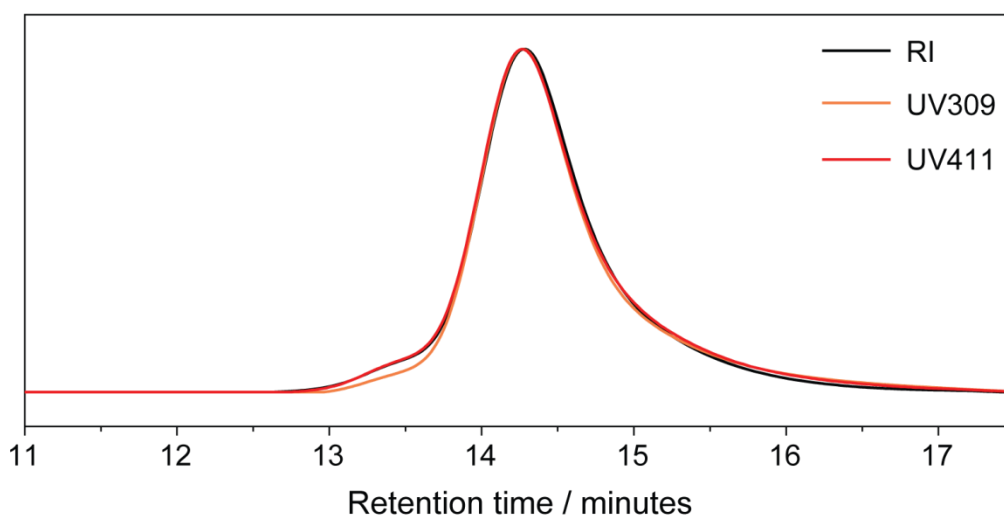


Figure S2. DMF SEC traces of **P1**. Black = refractive index (RI) detector. Orange = UV-vis detector at 309 nm. Red = UV-vis detector at 411 nm. Overlap of all three traces confirmed the incorporation of the trithiocarbonate and acridine groups at the polymer chain ends.

Intercalation studies for **P1-4**

The ability of the acridine-containing polymers to interact with double stranded DNA (dsDNA) by intercalation was assessed by titrations with calf thymus DNA (ctDNA) using UV-vis and linear dichroism (LD) spectroscopy. Intercalation was indicated by a decrease in absorbance of the main acridine peak around 411 nm and a concomitant red shift of the absorbance maxima, and a negative LD response (indicative of an interaction taking place perpendicular to the axis of the DNA double helix). For **P1** a red shift was observed (Figure S3), but the absorbance was observed to increase over the course of the first part of the titration rather than decrease. However, at higher base pair to acridine ratios the absorbance did decrease below its initial value, indicating that intercalation was taking place. A negative LD response was observed, confirming that intercalation was occurring (Figure S4). The increase in UV-vis absorbance was attributed to aggregation of the DNA–polymer complexes, which caused clouding of the solution. Figure S5 is a plot of absorbance at 550 nm (a wavelength commonly used for assessing the turbidity of a solution) *versus* concentration of polymer in a solution of ctDNA. Higher polymer concentrations lead to significant turbidity when **P1** is used; however, when poly(NIPAM) of a similar molecular weight but lacking the acridine end group is used, no turbidity is observed. The aggregation thus appears to be caused by the intercalation interaction between the polymer and the ctDNA.

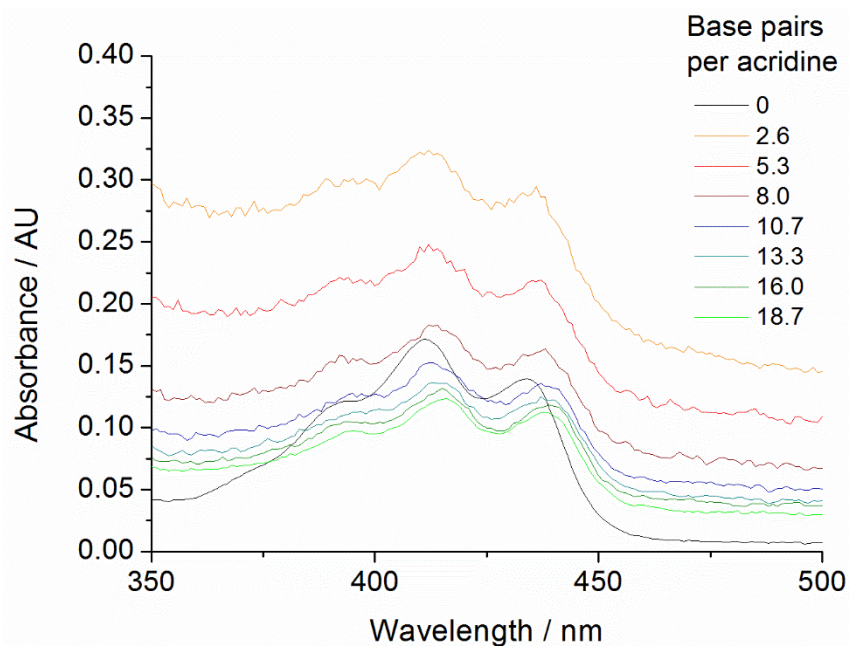


Figure S3. UV-vis absorbance spectra for mixtures of **P1** with ctDNA at various base pair to acridine group ratios.

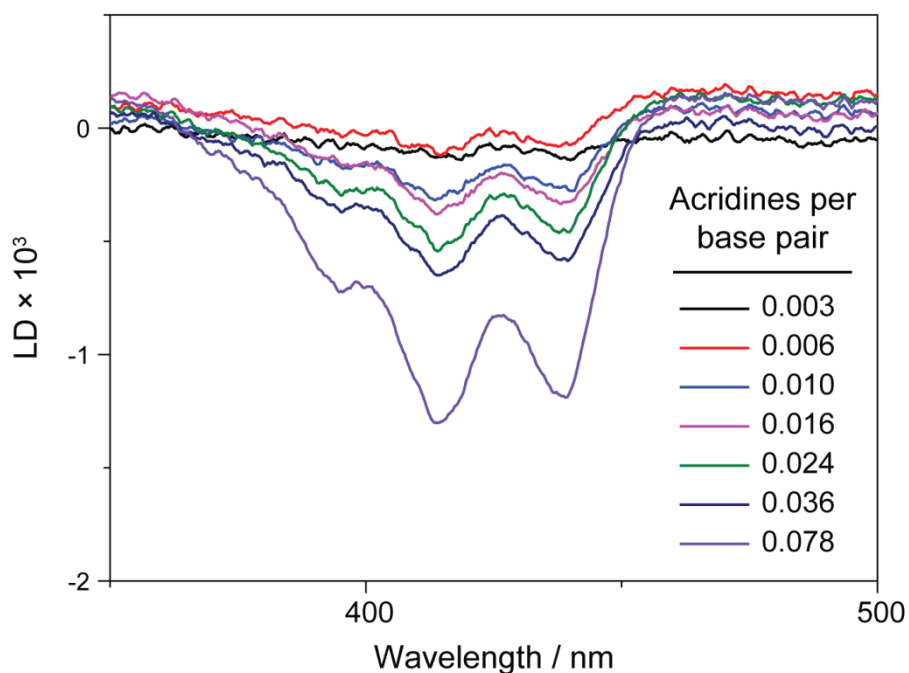


Figure S4. LD spectroscopy titration series showing the change in response as the ratio of **P1** to ctDNA is increased. The negative response indicates that the observed interaction is taking place perpendicular to the main axis of the dsDNA.

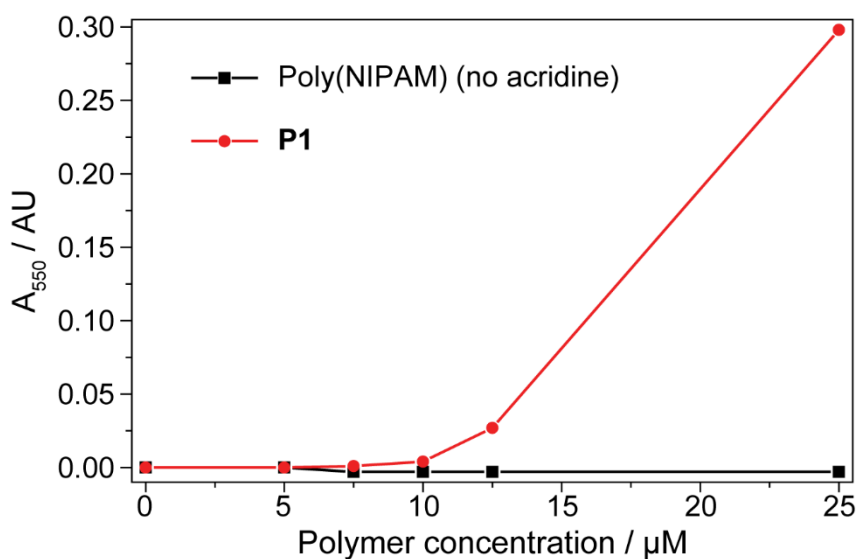


Figure S5. Plot of UV absorbance at 550 nm for a solution of ctDNA containing various concentrations of **P1** (red) and poly(NIPAM) of a similar molecular weight but lacking the acridine end group (black).

Intercalation was also observed by UV-vis spectroscopy for poly(4-AM) containing a terminal acridine group (**P2**), see Figure S6. In this case, aggregation was observed in the early stages of the titration, but was reversed once the number of base pairs per acridine had increased above approximately ten – Figure S7 shows a plot of the absorbance at 411 nm to illustrate this point. However, because this ‘aggregation regime’ (the region where the absorbance is greater than the initial value) was so large it proved impossible to extract an association constant (K_a) for this polymer’s interaction with dsDNA (see below).

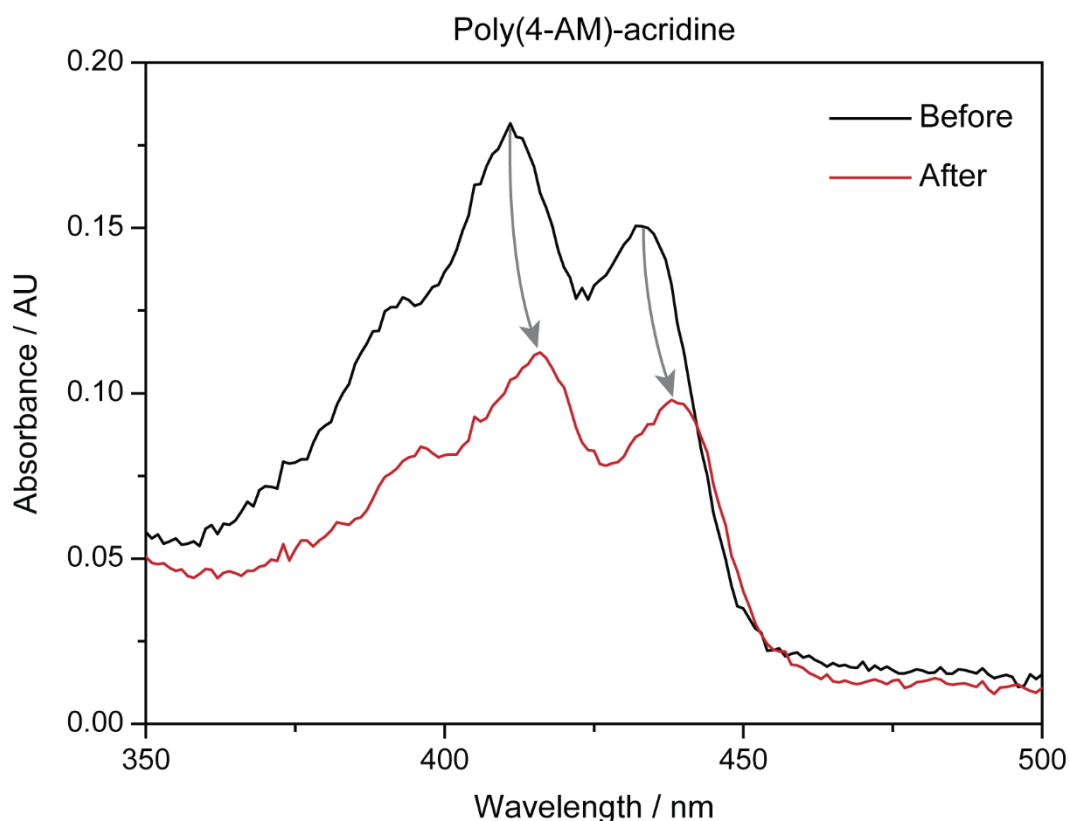


Figure S6. UV-vis spectra showing the effect of adding ctDNA to a solution of **P2** in water. Black = before addition; red = after addition.

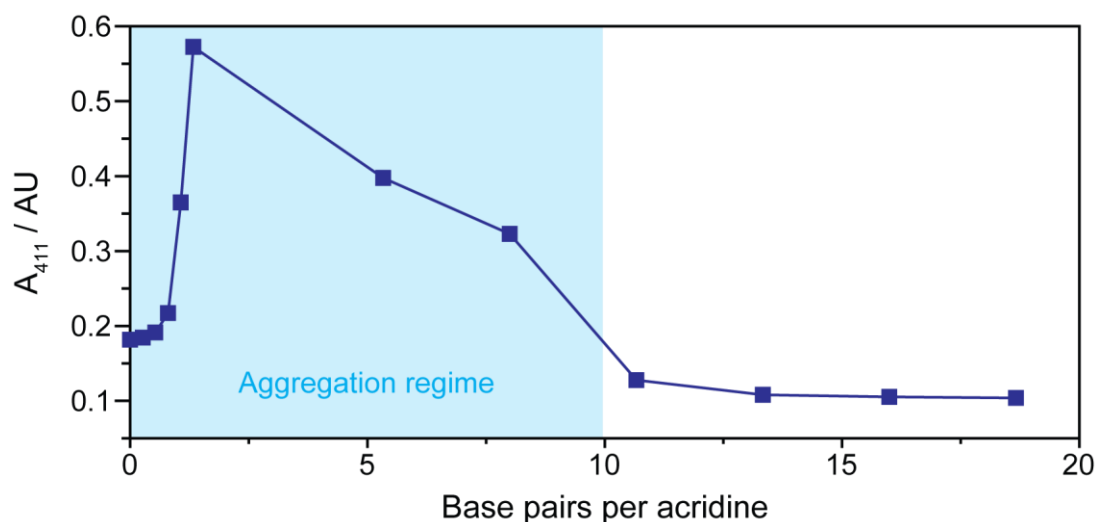


Figure S7. Progression of absorbance at 411 nm (A_{411}) with base pair/acridine ratio for **P2** interacting with ctDNA in water. The aggregation regime (blue highlighted region) is the range in which the A_{411} value was larger than the starting value, indicating clouding of the solution.

The aggregation regime for **P3a**, by contrast, was much narrower and a full titration series was obtained as depicted in Figure S8. To extract the association constant (K_a) for the interaction between **P3a** and ctDNA a series of 'delta' plots were first generated by subtracting the UV-vis spectrum at a particular titration point from the spectrum of the free polymer. The results are shown in Figure S9 and were used to identify the wavelength at which the greatest change in absorbance was observed (in this case 409 nm). Finally, the change in absorbance at 409 nm was plotted against the concentration of ctDNA and a non-linear least squares method used to fit

Equation S1 to the data, as shown in Figure S10 (see Experimental Section for a full explanation of the calculation). LD spectroscopy was also performed to confirm that the intercalation interaction was taking place – a significant negative response was observed (Figure S11). K_a was also extracted for **P3b** using an identical method.

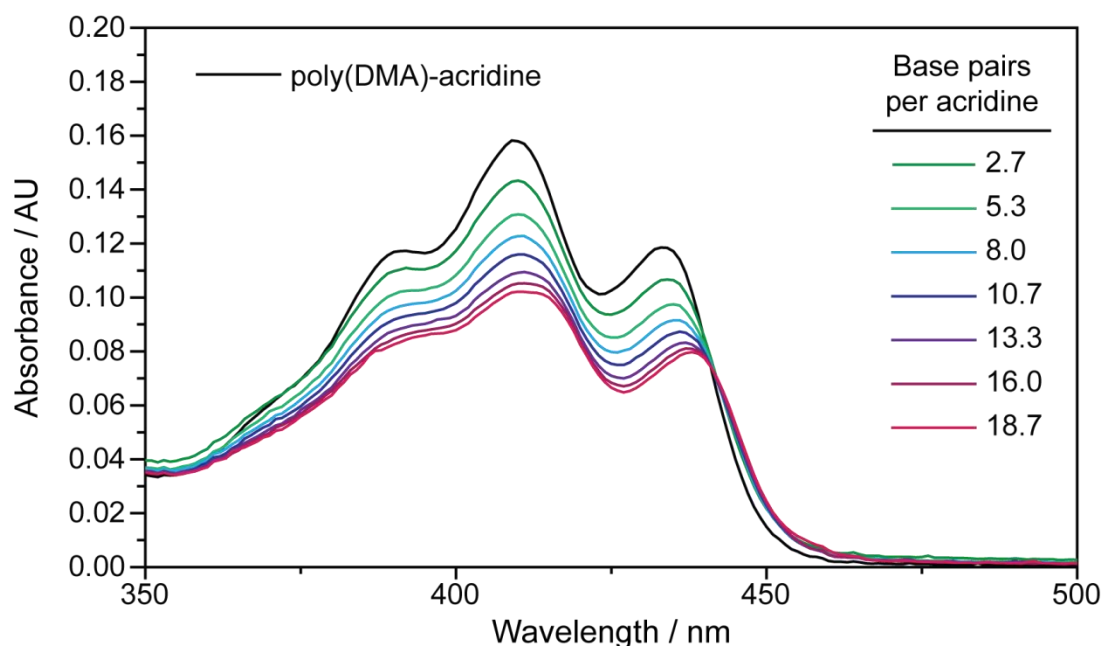


Figure S8. UV-vis spectroscopy titration series showing the effect of adding increasing amounts of ctDNA to a solution of **P3a** in water.

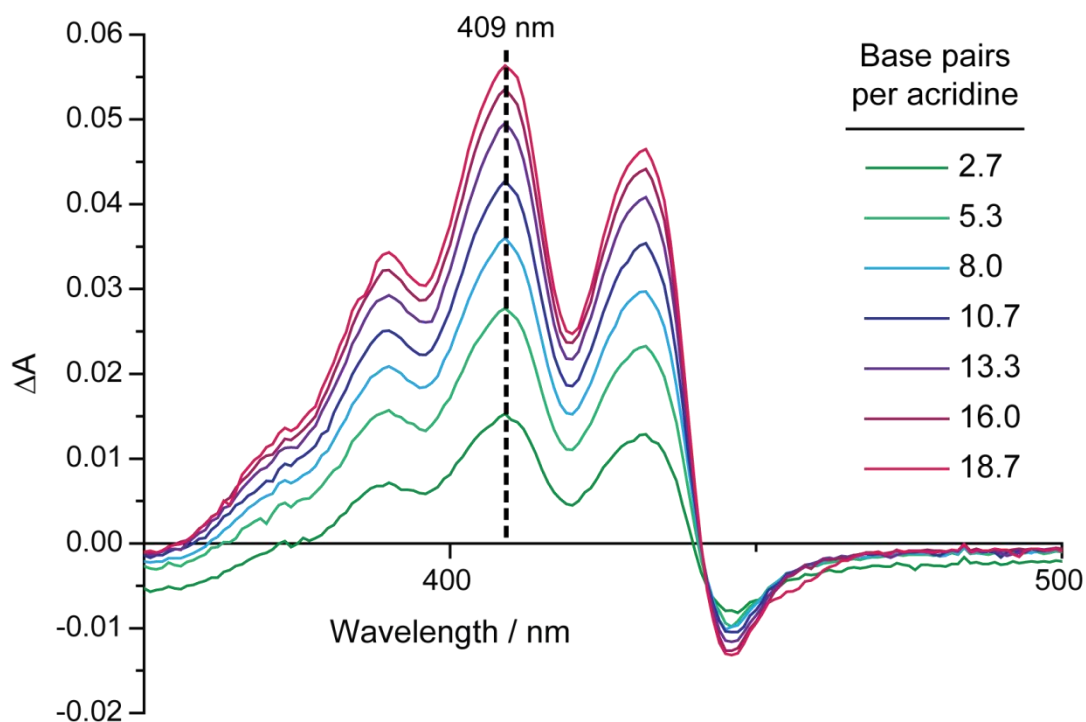


Figure S9. Delta plots for the interaction of **P3a** with ctDNA. Each spectrum was obtained by subtracting the UV-vis spectrum at that point during the titration from the original spectrum of free **P3a**. The greatest change in absorbance was observed at 409 nm, as indicated.

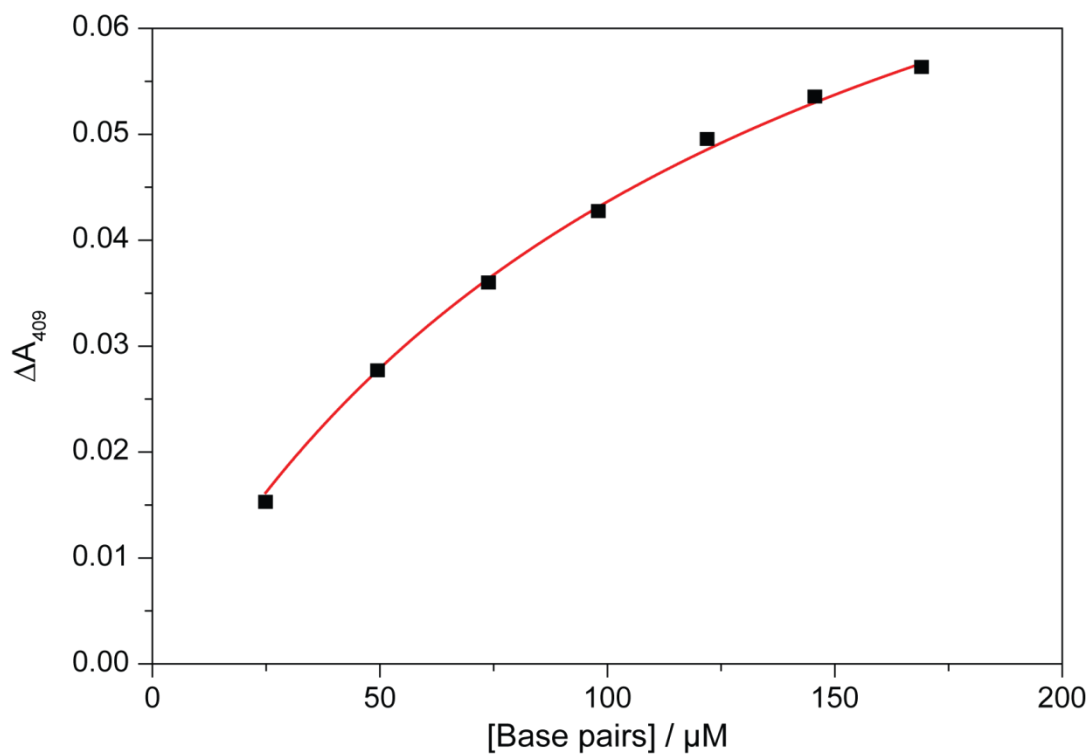


Figure S10. Plot of base pair concentration versus change in absorbance at 409 nm for **P3a** interacting with ctDNA. The red curve is from the fitted equation used to determine the equilibrium binding constant, K_a .

$$\Delta A = \frac{\Delta A_{max} K_a [\text{BP}]}{1 + K_a [\text{BP}]}$$

Equation S1. The relation between ΔA and free base pair concentration used to extract the association constant, K_a for the interaction between ctDNA and polymer containing an acridine end group, from UV-vis spectroscopy data.

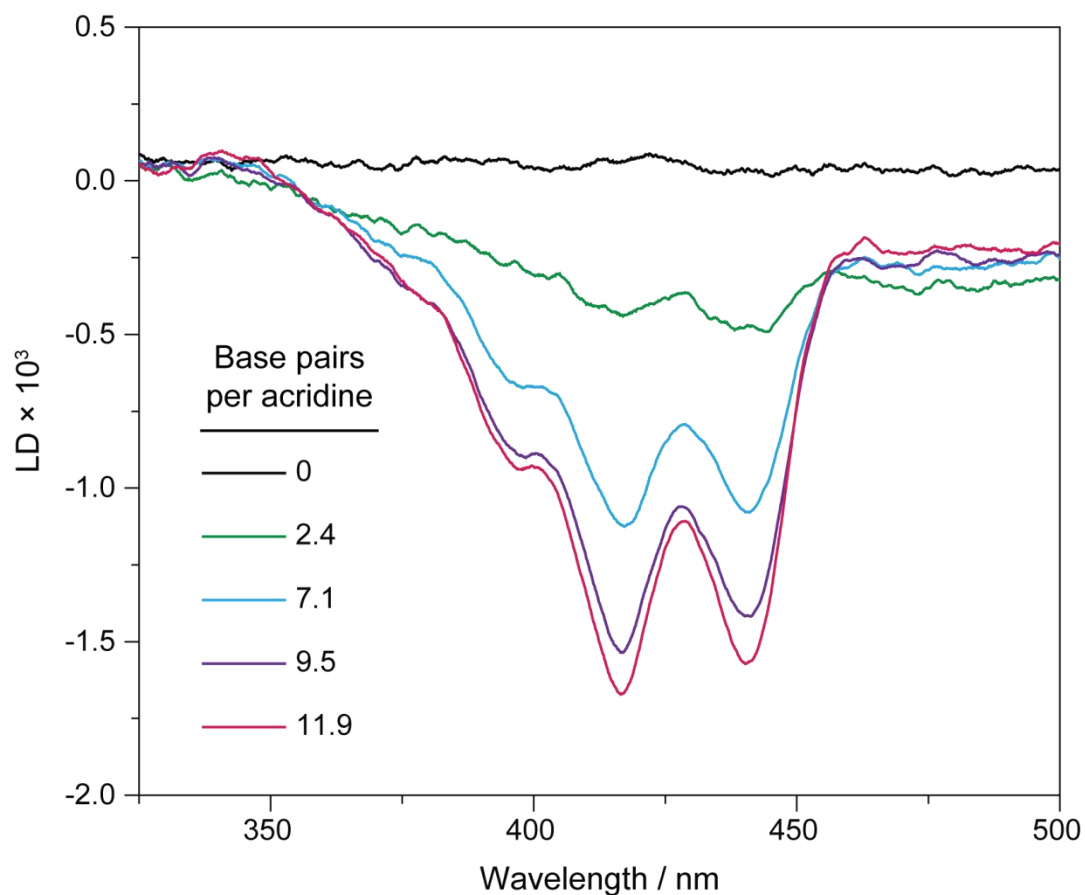


Figure S11. LD spectroscopy titration series measuring the interaction between **P3a** and ctDNA. The characteristic acridine peak shape emerged over the course of the titration and displayed a negative response, indicating that the measured interaction was taking place perpendicular to the direction of flow.

The interaction of poly(TEGA) containing an acridine end group (**P4**) with ctDNA was also investigated. However, it was found to be much weaker than that for **P3a** or **P3b**. Figure S12 compares the same points in the titration series for **P3a** and **P4** – much less hypo- and bathochromicity was observed for the latter, suggesting a weaker interaction. As for **P3a** and **P3b**, K_a was extracted for **P4** using the delta absorbance data and Equation S1. The fitted data are shown in Figure S13 and revealed a much lower K_a , although it should be noted that the quality of the fit in this case was not good, possibly indicating that competing interactions were disrupting the intercalation interaction.

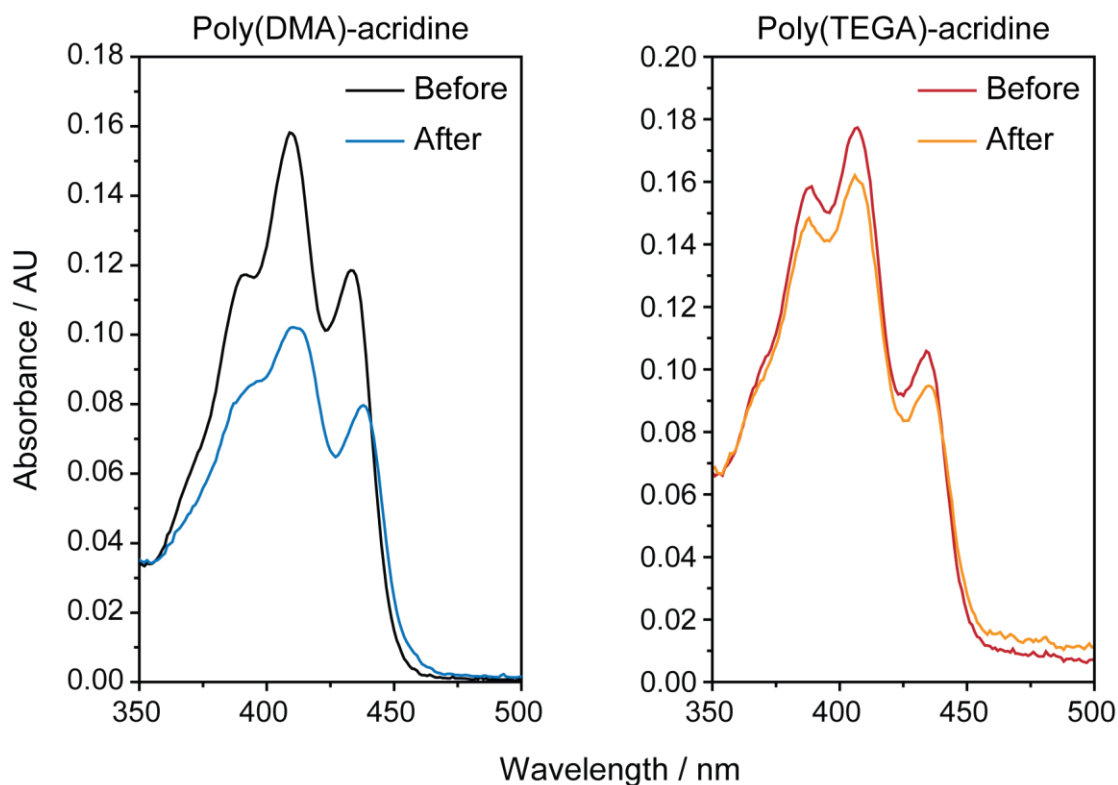


Figure S12. UV-vis spectra from the titration series of poly(DMA) (left) and poly(TEGA) (right) containing an acridine end-group against ctDNA.

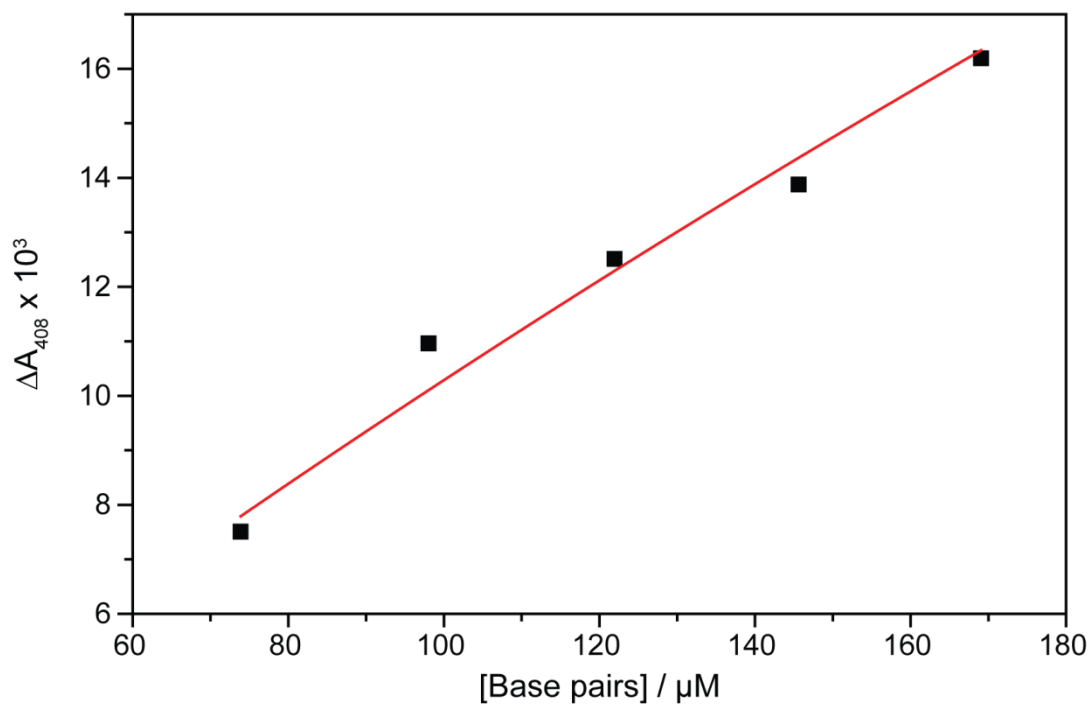


Figure S13. Data used to calculate K_a for the interaction of acridine-terminated poly(TEGA) with ctDNA. The red line is the result of a fit to Equation S1.

Use of short dsDNA to create hybrid particles

The short double stranded DNA (dsDNA) used in this study was assembled from the component strands (s1 and s1') and was termed **DNA-1**. Figure S14 shows native PAGE analysis of s1, s1' and

DNA-1. The successful formation of the latter was confirmed by the shift in migration distance of the main band, indicative of a higher molecular weight species.

The titration series with **P3a** was then repeated using **DNA-1** in place of ctDNA. The results are shown in Figure S15 and revealed very similar hypo- and bathochromicity effects, confirming that intercalation was still occurring with the shorter DNA strand.

After addition of the final aliquot of **DNA-1** in the UV-vis spectroscopy titration series, the solution was studied by dynamic light scattering (DLS). The results are shown in Figure S16 and showed the presence of a significant population of particles around 9 nm in diameter. However, there was also evidence of much larger aggregates (see intensity trace).

The solution was studied by atomic force microscopy (AFM) as described in the main paper. Large particles were observed in the dry state and the phase contrast image (Figure S17) suggested that the core and corona domains were composed of different materials (that is, each domain exhibited a different phase change suggesting differing degrees of interaction with the AFM tip).

Finally, the solution was studied by synchrotron small-angle X-ray scattering (SAXS). Cylindrical particles were observed as well as some aggregates (evidence by the rise in the curves above the fits at low q) at 10, 20, 30, 40 and 50 °C. Physical characteristics of the sample are presented in Table S2 and Table S3 and fits are presented in Figure S19. The core radius does not change with the temperature for the two fits and the shell thickness is dependent on the temperature: with a 31% and 14% increase for the fits of A and B respectively with increase from 10 to 50 °C. Interestingly, the shell SLD does not change significantly over this temperature increase, indicating that the density of the polymer remains relatively constant. Finally, the second fit confirms the accuracy of the first model as the core radius and shell thickness do not vary significantly. Length varies more between the two fits, however, due to some aggregation observed at low q , it is less accurate. The two fits give clear indication that the core and corona domains are composed of different materials (otherwise, a core-shell cylinder model would not fit the observed profiles).

Table S2. Physical characteristics of the hybrid particles. Length (20 nm), core SLD ($3.40 \cdot 10^{-6} \text{ \AA}^{-2}$) and water SLD were fixed during the fitting.

	Core radius (nm)	Shell thickness (nm)	Shell SLD (10^{-6} \AA^{-2})	Water SLD (10^{-6} \AA^{-2})
10 °C	2.23 ± 0.03	7.68 ± 0.07	9.354 ± 0.003	9.46
20 °C	2.25 ± 0.03	8.17 ± 0.06	9.360 ± 0.002	9.45
30 °C	2.23 ± 0.03	8.91 ± 0.08	9.356 ± 0.002	9.42
40 °C	2.26 ± 0.04	9.29 ± 0.12	9.341 ± 0.002	9.39
50 °C	2.40 ± 0.05	10.06 ± 0.20	9.306 ± 0.002	9.35

Table S3. Physical characteristics of the hybrid particles. Core SLD ($3.40 \cdot 10^{-6} \text{ \AA}^{-2}$), water SLD and shell SLD were fixed during the fitting with values obtained from the first fit (Table S2).

	Core radius (nm)	Shell thickness (nm)	Core length (nm)
10 °C	2.18 ± 0.02	7.22 ± 0.05	26.2 ± 0.7
20 °C	2.21 ± 0.01	7.55 ± 0.05	28.0 ± 0.6
30 °C	2.16 ± 0.01	7.86 ± 0.07	28.0 ± 0.8
40 °C	2.20 ± 0.01	7.88 ± 0.11	26.6 ± 0.8
50 °C	2.34 ± 0.02	8.29 ± 0.18	26.9 ± 1.2

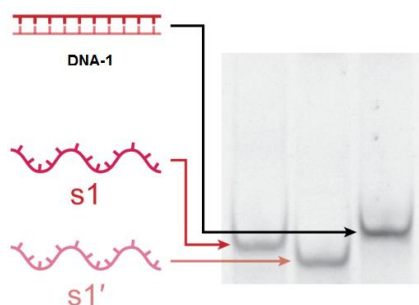


Figure S14. 15 % native PAGE analysis showing the formation of DNA-1 from s1 and s1'.

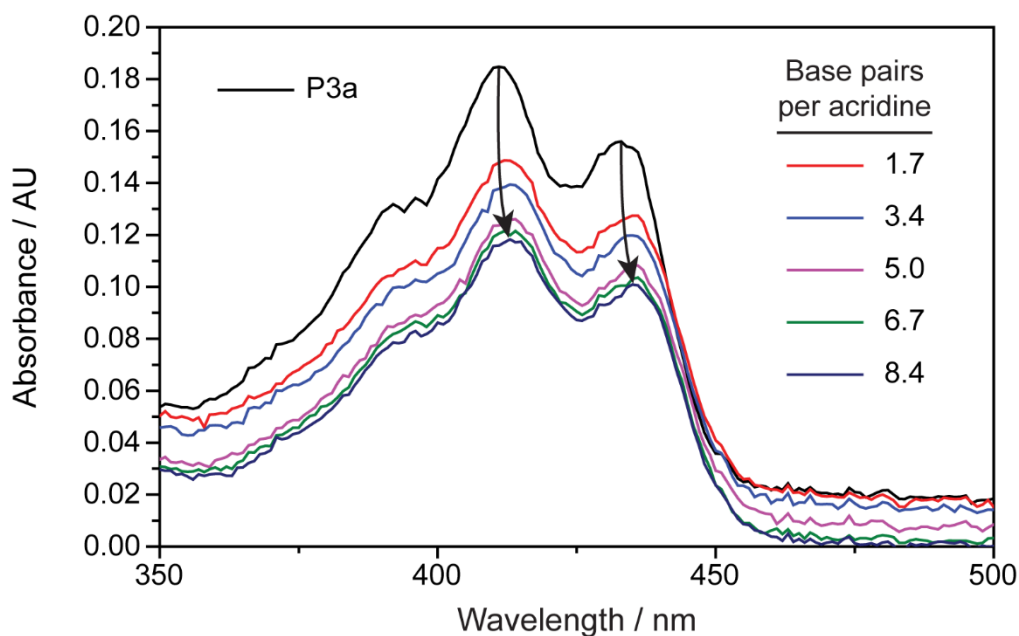


Figure S15. UV-vis spectroscopy titration series showing the effect of adding DNA-1 to a solution of P3a.

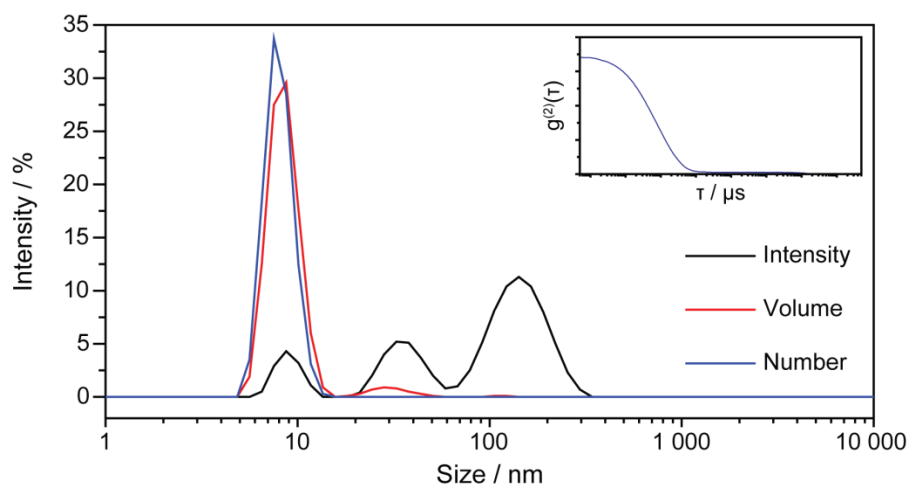


Figure S16. DLS analysis of a solution of **P3a** and DNA-1.

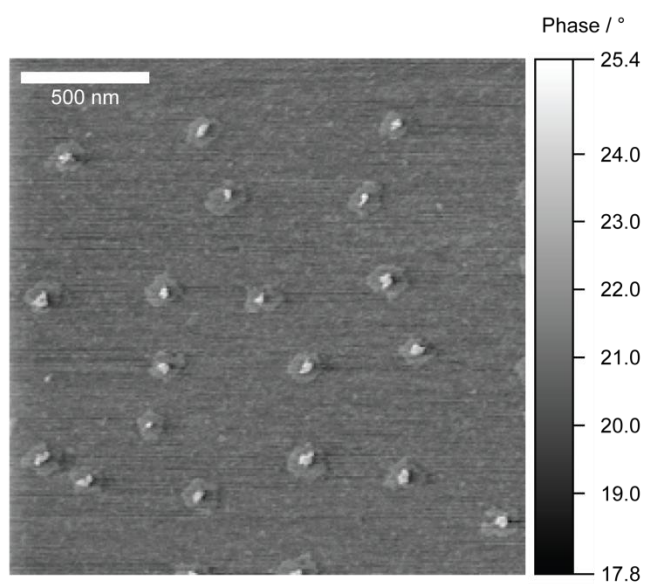


Figure S17. AFM phase contrast image of the particles formed by **P3a** in the presence of DNA-1 in water.

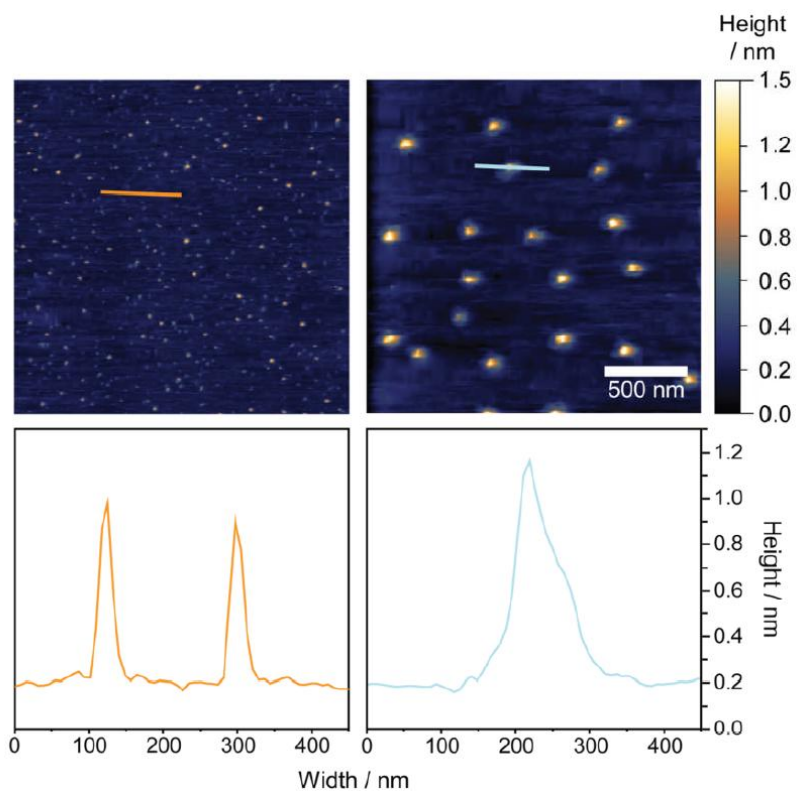


Figure S18. Comparison of the height plot profiles of DNA-1 (left) and DNA-1 in the presence of P3a (right). The AFM micrographs from which the data were taken are shown above the plots, with the location of the plot sample indicated by a solid line. Both images were taken at the same magnification.

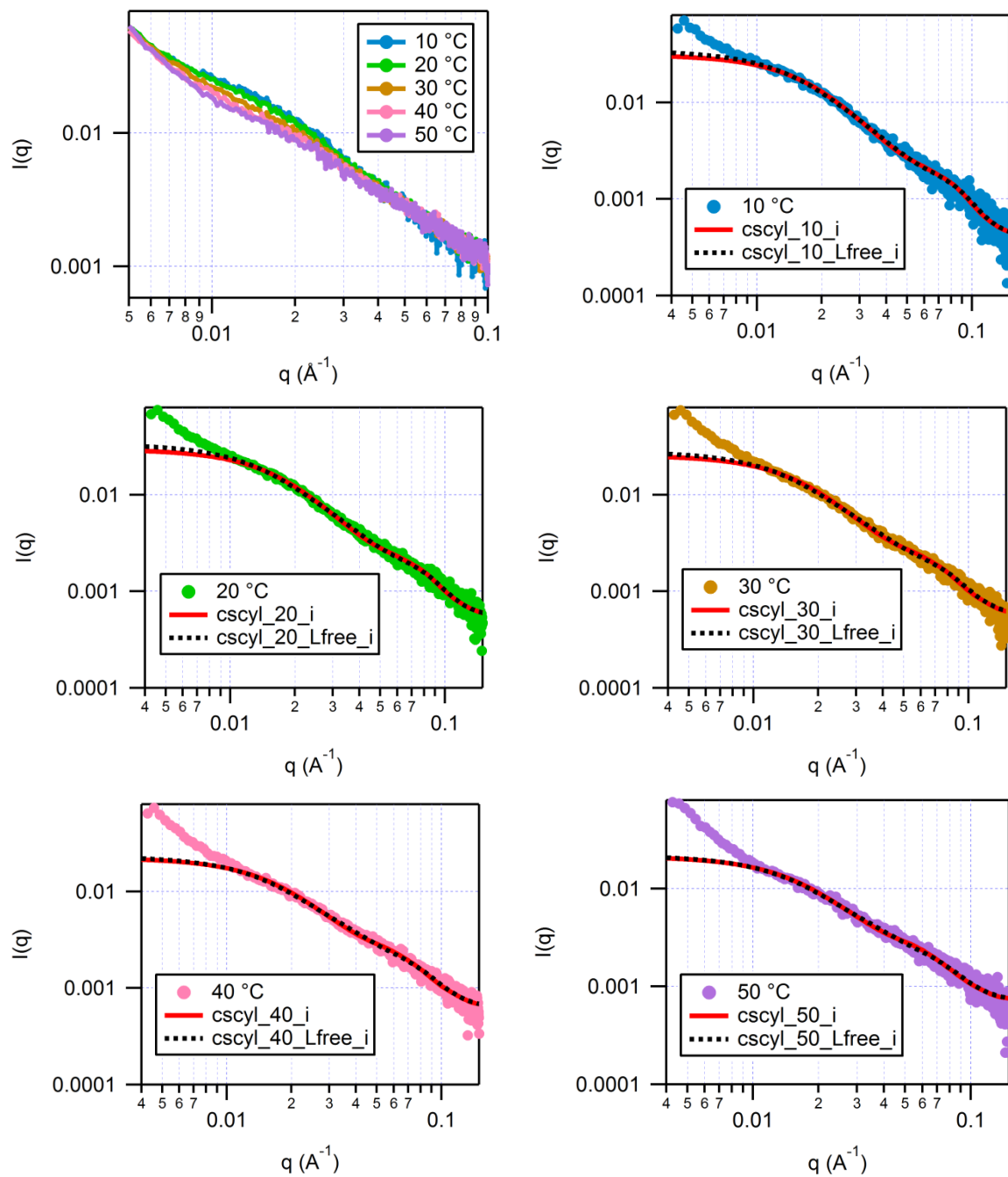


Figure S19. SAXS analysis of the hybrid particles at different temperatures. Experimental profiles and fittings with the core shell cylinder model for the five different temperatures with the length fixed (red line or not fixed black dotted line).

Experimental

Materials & Methods

AIBN was recrystallised twice from methanol prior to use. NIPAM was recrystallised from toluene prior to use. DMA and HEA were passed through a neutral alumina column to remove the radical inhibitor prior to use. TEGA was synthesised according to a previously published procedure.¹ 4-AM was distilled prior to use. LD spectroscopy was performed on a Jasco J-815 circular dichroism spectropolarimeter at room temperature using a custom-built 80 μ L Couette flow cell. 10 \times TM buffer consisted of 1 M Tris and 60 mM MgCl₂. DNA from calf thymus was purchased from Sigma-Aldrich and resuspended in 10 mM Tris-HCl, 1 mM EDTA solution prior to further use. The DNA strands s1 and s1' were purchased from Integrated DNA Technologies Ltd. and resuspended in 18 M Ω water to a final concentration of 200 μ M prior to use. The sequences of the DNA strands used were as follows:

s1 5'- AGG CAG TTG AGA CGA ACA TTC CTA AGT CTG AAA TTT ATC ACC CGC CAT AGT
 AGA CGT ATC ACC -3'

s1' 5'- GGT GAT ACG TCT ACT ATG GCG GGT GAT AAA TTT CAG ACT TAG GAA TGT TCG
 TCT CAA CTG CCT -3'

DMF SEC data were obtained in HPLC grade DMF containing 1 mg mL⁻¹ lithium bromide at 323 K, with a flow rate of 1.0 mL min⁻¹, on a set of two Varian PLgel 5 μ m Mixed-D columns (7.5 mm diameter), with guard column. SEC data were analysed using Cirrus SEC software calibrated using poly(methyl methacrylate) standards (690-271 400 Da) or poly(styrene) standards (162-371 100 Da). ¹H and ¹³C NMR spectra were recorded on Bruker DPX-300 or -400 spectrometers at 293 K. Chemical shifts are reported as δ in parts per million (ppm) and referenced to the residual solvent resonances (CDCl₃ ¹H: δ = 7.26 ppm; ¹³C δ = 77.16 ppm). IR measurements were collected on a PerkinElmer Spectrum 100 FT-IR spectrometer. Solid samples were crushed and then applied to the FTIR sensor; liquid samples were applied as a small droplet. UV-vis measurements were collected on a PerkinElmer Lambda 35 spectrometer using a Hellma TrayCell with a 1 mm path length adapter or with a quartz cell with a 1 cm path length (for titration measurements). DNA solution concentrations were determined using UV-vis absorption measurements at 260 nm and the known extinction coefficient supplied by the manufacturer, except in the case of calf thymus DNA, where an average base pair extinction coefficient of 6 600 M cm⁻¹ was used. ESI mass spectra were collected on a Bruker Esquire2000 ESI-MS machine using methanol as solvent. Native polyacrylamide gel electrophoresis (PAGE) was carried out with 1 \times Tris-Acetate EDTA (TAE) as running buffer at 4 °C and constant voltage of 200 V, loading with glycerol/bromophenol blue loading buffer. All gels were run using a Bio-Rad Mini-Protean Tetra System apparatus, and visualised using SYBR Gold nucleic acid stain, purchased from Invitrogen, under UV transillumination with a UVITEC UVIDOC HD2 gel documentation system. 1 \times TAE buffer consisted of 40 mM Tris-acetate and 1 mM EDTA. The native loading buffer consisted of 25% glycerol and 0.05% bromophenol blue in 1 \times TE buffer, and was diluted five-fold before use. Hydrodynamic diameters (D_h) and size distributions of nanoparticles were determined by DLS on a Malvern Zetasizer Nano ZS operating at 24 °C with a 4 mW He-Ne 63 nm laser module. Disposable plastic sizing microcuvettes were used. Measurements were made at a detection angle of 173° (back scattering), and the data analysed using Malvern DTS 5.02 software, using the multiple narrow modes setting. All measurements were made in triplicate, with at least 10 runs per measurement. AFM measurements were performed in tapping mode on a Multimode AFM with Nanoscope IIIA controller with Quadrex. Silicon AFM tips were used with nominal spring constant and resonance frequency of 3.5 Nm⁻¹ and 75 kHz (MikroMasch NSC18). Small-angle X-ray scattering (SAXS) measurements were carried on the SAXS/WAXS beamline at the

Australian Synchrotron facility at a photon energy of 11 keV. The samples in solution were run by using a 1.5 mm diameter quartz capillary. The capillary was held on a temperature controlled mount with temperature control via a water bath connected to a brass block which is part of the sample holder. 10, 20, 30, 40 and 50 °C were reached, and time was allowed for the sample to equilibrate. The measurements were collected at a sample to detector distance of 3.252 m to give a q range of 0.004 to 0.2 Å⁻¹, where q is the scattering vector and is related to the scattering angle (2θ) and the photon wavelength (λ) by the following equation:

$$q = \frac{4\pi \sin \theta}{\lambda}$$

All patterns were normalised to fixed transmitted flux using a quantitative beamstop detector. The scattering from a blank (H₂O) was measured in the same capillary and was subtracted for each measurement. The two-dimensional SAXS images were converted in one-dimensional SAXS profile ($I(q)$ versus q) by circular averaging, where $I(q)$ is the scattering intensity.

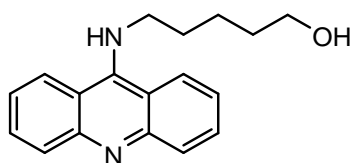
Acridin-9-ylmethyl dodecyl carbonotrithioate (**A**)

To a suspension of caesium carbonate (0.132 g, 0.40 mmol) in acetone (1 mL) was added dodecanethiol (88 µL, 0.37 mmol) and carbon disulfide (66 µL, 1.10 mmol) and the mixture stirred for 90 minutes. To the bright yellow suspension was added 9-bromomethylacridine (0.050 g, 0.19 mmol) and acetone (0.5 mL) and stirring continued for a further hour, after which time a further portion of 9-bromomethylacridine (0.050 g, 0.19 mmol) and acetone (0.5 mL) was added. The mixture was stirred for 5 hours at room temperature, then filtered and the solvent removed *in vacuo*. The crude residue was purified by recrystallisation from methanol to yield the product as orange crystals (0.066 g, 38%). ¹H NMR (400 MHz, CDCl₃) δ 8.26 (d, J = 9 Hz, 2H, ArH), 8.19 (d, J = 9 Hz, 2H, ArH), 7.80 (t, J = 8 Hz, 2H, ArH), 7.61 (t, J = 8 Hz, 2H, ArH), 5.57 (s, 2H, ArCH₂S), 3.44 (t, J = 7 Hz, 2H, SCH₂CH₂), 1.74 (quint, J = 7 Hz, 2H, SCH₂CH₂), 1.40 (m, 2H, SCH₂CH₂CH₂), 1.37-1.20 (br m, 18H, alkyl chain CH₂), 0.88 (t, J = 7 Hz, 3H, CH₃) ppm. ¹³C NMR (100 MHz, CDCl₃) δ 221.2 (C=S), 148.6, 130.6, 130.1, 126.8, 125.3, 123.8, 37.4, 33.7, 31.9, 29.6, 29.6, 29.5, 29.4, 29.1, 28.9, 28.0, 14.1 ppm. ESI MS calcd. for C₂₇H₃₅NS₃ [M+H]⁺ 470.2004; observed 470.2000. IR (ν_{\max} / cm⁻¹): 2918, 2849, 1470, 1093, 1062, 799, 755, 713.

RAFT polymerisations using CTA **A**

Polymerisations of NIPAM, styrene and methyl acrylate were attempted using CTA **A**; an example procedure follows. NIPAM (0.200 g, 1.77 mmol), **A** (0.008 g, 0.02 mmol) and AIBN (0.3 mg, 2 µmol) were all dissolved in DMF (0.4 mL) and transferred to an oven-dried ampoule. The solution was subjected to four freeze-pump-thaw cycles to remove oxygen, sealed under an atmosphere of nitrogen and placed in an oil bath preheated to 65 °C for 24 hours. Monomer conversion was measured by ¹H NMR and any isolated polymer product was analysed by SEC, eluting with THF.

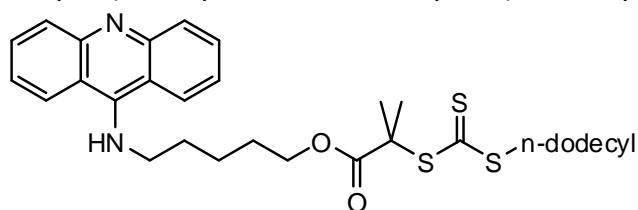
5-(acridin-9-ylamino)pentan-1-ol



5-(acridin-9-ylamino)pentan-1-ol was synthesised as previously reported.² 9-Chloroacridine (0.3350 g, 1.57 mmol) and 5-amino-1-pentanol (0.4044 g, 3.92 mmol) were dissolved in anhydrous DMF (3.35 mL). The solution was thoroughly degassed by three successive freeze-pump-thaw cycles,

sealed under nitrogen and heated to 100 °C for 5 hours. The reaction was allowed to cool and then water (20 mL) was added and the organic components extracted into dichloromethane (3 × 20 mL). The organic layer was washed with saturated NaHCO₃ solution (20 mL), and brine (20 mL), and dried (Na₂SO₄). The drying agent was removed by filtration and washed on the filter with dichloromethane (2 × 10 mL). The solvent was removed *in vacuo* to afford the product as an orange solid (0.3717 g, 85%). ¹H NMR (300 MHz, CDCl₃) δ 8.09 (d, *J* = 9 Hz, 2H, ArH), 8.03 (d, *J* = 10 Hz, 2H, ArH), 7.64 (t, *J* = 8 Hz, 2H, ArH), 7.34 (t, *J* = 8 Hz, 2H, ArH), 3.84 (t, *J* = 7 Hz, 2H, CH₂OH), 3.68 (t, *J* = 6 Hz, 2H, CH₂NH), 1.84 (quint, *J* = 7 Hz, 2H, CH₂CH₂NH), 1.68-1.52 (m, 4H, CH₂CH₂CH₂OH) ppm. ¹³C NMR (100 MHz, CDCl₃) δ 130.44 (ArC), 128.01 (ArC), 123.05 (ArC), 123.02 (ArC), 115.99 (ArC), 62.35 (CH₂OH), 50.51 (CH₂NH), 32.09 (CH₂CH₂NH), 31.18 (CH₂CH₂OH), 23.23 (CH₂CH₂CH₂OH) ppm. ESI MS calcd. for C₁₈H₂₀N₂O [M+H]⁺ 281.2; observed 281.2. IR (ν_{max} / cm⁻¹): 3328, 2912, 2850, 1559, 1507, 1430, 1262, 1076, 754, 739.

5-(acridin-9-ylamino)pentyl 2-(dodecylthiocarbonothioylthio)-2-methylpropanoate, **1**



DDMAT (0.260 g, 0.71 mmol), 5-(acridin-9-ylamino)pentan-1-ol (0.200 g, 0.71 mmol), EDCI (0.137 g, 0.71 mmol) and DMAP (0.044 g, 0.36 mmol) were dissolved in a mixture of CHCl₃ (5 mL) and DCM (5 mL) and the solution bubbled with nitrogen for 30 minutes. The reaction was then sealed under nitrogen and stirred at room temperature for 24 hours, after which a further portion of EDCI (0.1368 g, 0.71 mmol) was added and the reaction allowed to stir for a further 24 hours. The solvent was removed *in vacuo*. Saturated NaHCO₃ solution (15 mL) was added and the products were extracted into DCM (3 × 15 mL). The organic layer was washed with water (2 × 20 mL), and brine (20 mL) and then dried (Na₂SO₄). The drying agent was removed by filtration and washed on the filter with DCM (2 × 10 mL). The solvent was removed from the filtrate *in vacuo* and the residue taken up in a mixture of 9:1 EtOAc/MeOH (15 mL) to precipitate the acridine starting material and EDCI by-product, which were then removed by filtration. The solvent was again removed *in vacuo* and the residue purified by silica gel column chromatography, eluting with EtOAc/MeOH (40:1) and triethylamine (0.1%). **1** was isolated (R_f 0.15) as a very viscous orange liquid (0.2353 g, 53%). ¹H NMR (300 MHz, CDCl₃) δ 8.09 (d, *J* = 9 Hz, 2H, ArH), 7.96 (d, *J* = 9 Hz, 2H, ArH), 7.56 (m, 2H, ArH), 7.31 (m, 2H, ArH), 6.02 (br s, 1H, NH), 4.13 (t, *J* = 6 Hz, 2H, CH₂O), 3.87 (t, *J* = 7 Hz, 2H, NHCH₂), 3.19 (t, *J* = 7 Hz, 2H, SCH₂), 1.90 (m, 2H, NHCH₂CH₂), 1.73 (m, 2H, CH₂CH₂O), 1.68 (s, 6H, C(CH₃)₂), 1.57 (m, 2H, NHCH₂CH₂CH₂), 1.45 (m, 2H, SCH₂CH₂), 1.15-1.35 (br m, 18H, SCH₂CH₂(CH₂)₁₈CH₃), 0.87 (t, *J* = 7 Hz, 3H, S(CH₂)₁₁CH₃) ppm. ¹³C NMR (100 MHz, CDCl₃) δ 221.7 (C=S), 173.0 (C=O), 152.1, 147.8, 130.5, 127.9, 123.2, 123.1, 116.0, 65.7, 56.0, 50.6, 37.0, 32.0, 31.1, 29.7, 29.6, 29.5, 29.4, 29.1, 28.9, 28.1, 27.9, 25.4 (C(CH₃)₂), 23.5, 22.7, 14.2 ((CH₂)₁₁CH₃) ppm [1 signal due to C's 12 missing because of overlap]. ESI MS calcd. for C₃₅H₅₀N₂O₂S₃ [M+H]⁺ 627.3107; observed 627.3108. IR (ν_{max} / cm⁻¹): 2922, 2852, 1731, 1559, 1465, 1258, 1155, 1126, 1062, 814, 752.

Measurement of the extinction coefficient

To measure the extinction coefficient the following dilutions of the molecule of interest were made in either acetonitrile or water: 5, 7.5, 10, 25, 50, 75 and 100 μM. The absorbance at the wavelength under investigation was then recorded for each solution and absorbance plotted *versus* concentration. Using the equation

$$A = \epsilon cl$$

where A is the absorbance, ϵ is the extinction coefficient, c is the concentration and l is the path length of the UV-vis spectrometer cell, ϵ could be determined by plotting A versus c for a series of known c values and taking the gradient of the resultant line of best fit.

Measurement of reaction kinetics for the polymerisation of NIPAM with **1**

1 (55 mg, 0.09 mmol), NIPAM (1 g, 8.84 mmol) and AIBN (2 mg, 0.01 mmol) were dissolved in DMF (1.5 mL) and the mixture degassed by three successive freeze-pump-thaw cycles, then sealed under nitrogen. A 100 μ L aliquot was removed every thirty minutes and analysed by ^1H NMR spectroscopy and DMF SEC. M_n values were estimated using PMMA calibration standards.

Poly(NIPAM)

1 (55.4 mg, 0.09 mmol), NIPAM (1 g, 8.84 mmol) and AIBN (1.5 mg, 0.01 mmol) were mixed in DMF (1.5 mL) and the solution degassed by three successive freeze-pump-thaw cycles. After warming to room temperature and sealing under an atmosphere of nitrogen, the reaction vessel was placed in an oil bath heated to 65 °C for 2.5 hours. The polymer solution was diluted with THF (~1 mL) and precipitated into diethyl ether (300 mL) cooled with dry ice, and collected by filtration to yield the product as a yellow solid (370.9 mg, 55%^{*}), which was then analysed by DMF SEC using PMMA calibration standards (M_n 6.3 kDa, \bar{D} 1.15). ^1H NMR (CDCl_3 , 400 MHz) 8.22 (m, 2H, acridine H), 8.07 (m, 2H, acridine H), 7.71 (m, 2H, acridine H), 7.37 (m, 2H, acridine H), 7.60-5.60 (br m, PNIPAM NH), 3.98 (br s, PNIPAM $\text{CH}(\text{CH}_3)_2$), 3.32 (m, 2H, SCH_2), 2.6-0.8 (br m, PNIPAM backbone H), 1.12 (br s, PNIPAM $\text{CH}(\text{CH}_3)_2$), 0.87 (t, $J = 7$ Hz, 3H, $\text{S}(\text{CH}_2)_{11}\text{CH}_3$) ppm.

Poly(DMA)

Two molecular weights of poly(DMA) were synthesised. What follows is an example procedure. **1** (20.0 mg, 32 μ mol), DMA (327.0 mg, 3.3 mmol) and AIBN (0.5 mg, 3 μ mol) were mixed in 1,4-dioxane (1.26 mL) and the solution degassed by three successive freeze-pump-thaw cycles. After warming to room temperature and sealing under an atmosphere of nitrogen, the reaction vessel was placed in an oil bath heated to 65 °C for four hours. The polymer was precipitated from pet. ether 40-60 (100 mL) cooled in an ice bath and allowed to settle. The solvent was decanted and the solid re-dissolved in 1,4-dioxane (2 mL), then precipitated again into pet. ether 40-60 (100 mL) cooled in an ice bath. The mixture was centrifuged and the solvent decanted to afford the product as a yellow solid (98 mg, 46%[†]), which was analysed by DMF SEC using PMMA calibration standards (M_n 6.7 kDa, \bar{D} 1.13). ^1H NMR (CDCl_3 , 400 MHz) 8.19 (br m, 2H, acridine H), 8.09 (br m, 2H, acridine H), 7.67 (br t, 2H, acridine H), 7.35 (br m, 2H, acridine H), 4.20-3.80 (br m, 4H, end group NCH_2 and $(\text{CH}_3)_2\text{CO}_2\text{CH}_2$), 3.32 (br m, 2H, SCH_2), 3.25-2.20 (br m, PDMA $\text{CHCON}(\text{CH}_3)_2$), 2.15-0.95 (br m, PDMA backbone H), 0.78 (t, $J = 7$ Hz, 3H, $\text{S}(\text{CH}_2)_{11}\text{CH}_3$) ppm.

Poly(TEGA)

1 (20.0 mg, 32 μ mol), TEGA (651.4 mg, 3.2 mmol) and AIBN (0.5 mg, 3 μ mol) were mixed in DMF (1.3 mL) and the solution degassed by three successive freeze-pump-thaw cycles. After warming to room temperature and sealing under an atmosphere of nitrogen, the reaction vessel was placed in an oil bath heated to 65 °C for seven hours. 18 M Ω water (9 mL) was added and the solution dialysed against water (MWCO 1 000 Da) for two days, incorporating five water changes. The product was isolated by freeze-drying as a yellow solid (308 mg, 66%[‡]), which was analysed by DMF SEC using

* Based on 62% monomer conversion as assessed by ^1H NMR spectroscopy at the end of the polymerisation.

† Based on 65% monomer conversion as assessed by ^1H NMR spectroscopy at the end of the polymerisation.

‡ Based on 72% monomer conversion as assessed by ^1H NMR spectroscopy at the end of the polymerisation.

PMMA calibration standards (M_n 10.1 kDa, \bar{D} 1.22). ^1H NMR (CDCl_3 , 400 MHz) 8.18 (m, 2H, acridine H), 7.68 (m, 2H, acridine H), 7.37 (br t, 2H, acridine H), 4.17 (br s, PTEGA CO_2CH_2), 3.63 (br s, PTEGA OCH_2), 3.53 (br t, PTEGA $\text{CO}_2\text{CH}_2\text{CH}_2$), 3.37 (br s, PTEGA CH_3), 2.31 (br m, PTEGA CHCO_2), 2.10-1.00 (br m, PTEGA backbone H), 0.87 (t, $J = 7$ Hz, 3H, $\text{S}(\text{CH}_2)_{11}\text{CH}_3$) ppm.

Poly(4-AM)

1 (44.4 mg, 71 μmol), 4-AM (0.5 g, 3.5 mmol) and AIBN (1.2 mg, 7 μmol) were mixed in 1,4-dioxane (1.5 mL) and the solution degassed by three successive freeze-pump-thaw cycles. After warming to room temperature and sealing under an atmosphere of nitrogen, the reaction vessel was placed in an oil bath heated to 70 °C for five hours. The solution was diluted with 18 M Ω water (50 mL) and dialysed against deionised water, incorporating five water changes. The product was isolated by freeze-drying as a pale yellow solid (335.0 mg, 84%[§]), which was analysed by DMF SEC using PMMA calibration standards (M_n 8.4 kDa, \bar{D} 1.15). ^1H NMR (CDCl_3 , 400 MHz) 8.12 (br m, 2H, acridine H), 8.03 (br s, 2H, acridine H), 7.64 (br s, 2H, acridine H), 7.33 (br m, 2H, acridine H), 4.20-3.00 (br m, P4-AM $\text{NCH}_2\text{CH}_2\text{O}$), 2.90-2.20 (br m, P4-AM CHC=O), 2.20-1.00 (br m, P4-AM backbone H), 0.87 (t, $J = 7$ Hz, 3H, $\text{S}(\text{CH}_2)_{11}\text{CH}_3$) ppm.

Measurement of the association constant, K_a

This section details the derivation of the equations used to calculate the association constant for the acridine-containing polymers with ctDNA.

The total concentrations of DNA base pairs and acridine in the solution ($[\text{BP}]_0$ and $[\text{Acr}]_0$) are related to the concentrations of free acridine, free base pairs and base pair–acridine complex as shown in Equation S2. Definition of the total concentration of acridine ($[\text{Acr}]_0$) and base pairs ($[\text{BP}]_0$) in terms of the concentrations of free acridine, free base pairs and base pair–acridine complex.

$$[\text{Acr}]_0 = [\text{Acr}] + [\text{BP-Acr}]$$

$$[\text{BP}]_0 = [\text{BP}] + [\text{BP-Acr}]$$

Equation S2. Definition of the total concentration of acridine ($[\text{Acr}]_0$) and base pairs ($[\text{BP}]_0$) in terms of the concentrations of free acridine, free base pairs and base pair–acridine complex.

The mole fraction, $f_{\text{BP-Acr}}$, of base pair–acridine complex in solution is defined according to Equation S3. Note that $f_{\text{BP-Acr}}$ is defined in terms of the concentration of free acridine, not free DNA. This is because, in the case of the UV-vis titrations above, the acridine concentration was kept almost constant throughout the experiment, which simplifies the analysis.

$$f_{\text{BP-Acr}} = \frac{[\text{BP-Acr}]}{[\text{Acr}] + [\text{BP-Acr}]} = \frac{[\text{BP-Acr}]}{[\text{Acr}]_0}$$

Equation S3. Definition of the mole fraction, $f_{\text{BP-Acr}}$, of base pair–acridine complex present in solution.

Using Equation S2 and Equation S3, the mole fraction can then be re-written as shown in Equation S4.

$$f_{\text{BP-Acr}} = \frac{K_a[\text{BP}]}{1 + K_a[\text{BP}]}$$

Equation S4. Expression of the mole fraction of base pair–acridine complex present in solution as a function of the association constant and the concentration of free base pairs.

The mole fraction of base pair–acridine complex is related to its concentration by Equation S5.

[§] Based on 80% monomer conversion as assessed by ^1H NMR spectroscopy at the end of the polymerisation.

$$[\text{BP-Acr}] = f_{\text{BP-Acr}}[\text{Acr}]_0$$

Equation S5. Relation of the mole fraction of base pair–acridine complex to its concentration.

The observed change in absorbance, ΔA , can be written as shown in Equation S6, where $\epsilon_{\Delta\text{BP-Acr}}$ is the 'delta extinction coefficient' – essentially the difference between the extinction coefficients of the free acridine and the acridine when complexed to a base pair.

$$\Delta A = \epsilon_{\Delta\text{BP-Acr}}[\text{BP-Acr}]$$

Equation S6. Expression of the observed change in UV-vis absorbance (ΔA) in terms of the concentration of the base pair–acridine complex and the delta extinction coefficient.

By substituting in Equation S4 and Equation S5, and noting that $\Delta A_{\text{max}} = \epsilon_{\Delta\text{BP-Acr}}[\text{Acr}]_0$, an expression for ΔA in terms of K_d and free base pair concentration can then be obtained, as shown in Equation S1.

UV-vis spectroscopy titrations to determine K_d

A 1.5 mL solution of acridine-containing polymer (**P1-4**) was made up at 20 μM (calculated using the extinction coefficient of the acridine group) by diluting a 1 mM acetonitrile stock solution with 18 M Ω water. The sample was heated to 30 °C within the UV-vis spectrometer (with stirring) and the UV-vis spectrum recorded. DNA (10 μL , 5 mM concentration of base pairs in 1 \times TM buffer) was added and the mixture allowed to equilibrate for two minutes before repeating the UV-vis measurement. This process was repeated until the desired amount of DNA had been added. The data were analysed and manipulated using OriginLab 8.5 graphing and analysis software, using a non-linear least squares method with Equation S1 to calculate K_d .

LD spectroscopy

A 1.5 mL solution of acridine-containing polymer (**P1-4**) was made up at 20 μM (calculated using the extinction coefficient of the acridine group) by diluting a 1 mM acetonitrile stock solution with 18 M Ω water. The LD spectrum was then recorded. ctDNA (1 μL , 5 mM in 1 \times TE buffer) and 18 M Ω water (49 μL) were added and the mixture shaken by hand for one minute before repeating the LD measurement. Measurements were also made of solutions to which had been added 2, 3, 4, 5, 10, 20, 30, 40 and 50 μL of the ctDNA solution. In each case an appropriate amount of 18 M Ω water was added so that the total volume of liquid added to the polymer solution was 50 μL .

Assembly of **DNA-1**

The double stranded **DNA-1** was assembled from the component strands (s_1 and s_1') as follows. s_1 (50 μL , 200 μM in water) and s_1' (50 μL , 200 μM in water) were mixed with 18 M Ω water (12.5 μL) and 10 \times TM buffer (12.5 μL). The solution was heated to 95 °C for twenty minutes and then left to cool slowly in the heating block to room temperature. Formation of the double helix was confirmed by 15% native PAGE analysis.

AFM

A solution of the **DNA-1–P3a** complex was studied by AFM as follows. **P3a** (1.5 mL, 20 μM in water) was mixed with **DNA-1** (50 μL , 80 μM in 1 \times TM buffer) and the mixture allowed to equilibrate for two minutes. The solution was diluted one hundred-fold with 18 M Ω water and immediately deposited onto freshly-cleaved mica and allowed to air-dry at room temperature. The sample was then placed inside the atomic force microscope and analysed in tapping mode. Solutions of **DNA-1**, **P3a** and **DNA-1** in the presence of poly(DMA) without an acridine end group were also analysed using this procedure.

SAXS

The function used for the fitting from the NCNR package was “CoreShellCylinder”. Scattering length densities (SLD) were calculated using the “Scattering Length Density Calculator” provided by the NIST Center for Neutron Research. SLD for DNA was initially stated as $3.40 \times 10^{-6} \text{ \AA}^{-2}$, this average value was found on the following website: www.ncnr.nist.gov/staff/hammouda/distance-learning/chapter-47.pdf. SLD for water were dependant on temperature as the water density varies with temperature and stated for the fits. SLD for the PDMA shell was initially stated at $8.92 \times 10^{-6} \text{ \AA}^{-2}$. Two different fits were done for each temperature experiment. The first one (“cscyl”) was done with the length of the assembly (20 nm), the core SLD ($3.40 \times 10^{-6} \text{ \AA}^{-2}$) and the solvent SLD (9.46, 9.45, 9.42, 9.39 and $9.35 \times 10^{-6} \text{ \AA}^{-2}$ for 10, 20, 30, 40 and 50 °C respectively) fixed. The core radius, the shell thickness and the shell SLD were thus free to evolve. The second fit (“cscyl_Lfree”) was done by holding the three SLDs with values from the first fit. The three dimensions of the nanostructure were let free to evolve (core radius and length and shell thickness).

Zeta potential

The DNA nanoconstructs shown in Figure S17, all at the same concentration were examined in a range of different salt solutions.

150 mM NaCl: -11.2 mV

5 mM KCl: -19.88 mV

30 mM carbonate buffer: -26.13 mV

Water: -26.4 Mv

References

1. J.-H. Ryu, R. Roy, J. Ventura and S. Thayumanavan, *Langmuir*, 2010, 26, 7086-7092.
2. S. Imoto, T. Hirohama and F. Nagatsugi, *Bioorg. Med. Chem. Lett.*, 2008, 18, 5660-5663.